

Article

The Important Role of Denitrifying Exoelectrogens in Single-Chamber Microbial Fuel Cells after Nitrate Exposure

Xiaojun Jin ^{1,*}, Wenyi Wang ², Zhuo Yan ³ and Dake Xu ^{1,*}¹ College of Materials Science and Engineering, Northeastern University, Shenyang 110819, China² College of Life and Health Sciences, Northeastern University, Shenyang 110819, China; 2001394@stu.neu.edu.cn³ College of Artificial Intelligence, Shenyang Aerospace University, Shenyang 110136, China; zhuoy@sau.edu.cn

* Correspondence: jinxiaojun@mail.neu.edu.cn (X.J.); xudake@mail.neu.edu.cn (D.X.); Tel.: +86-186-4005-0690 (X.J.); +86-186-2430-1199 (D.X.)

Abstract: Wastewater treatment using microbial fuel cells (MFCs) is a potentially useful technology due to its low cost, environmental friendliness, and low sludge production. In this study, a single-chambered air cathode MFC (SCMFC) was developed and investigated regarding its performance and microbial community evolution following nitrate exposure. During long-term operation, diverse denitrifiers accumulated on the electrodes to form a denitrifying MFC (DNMFC) with stable activity for nitrate reduction. The DNMFC presented considerably higher electroactivity, stability, and denitrification rates than the SCMFC. Though energy recovery decreased in the DNMFC by partial organics utilized for heterotrophic denitrification, the electron transfer efficiency increased. *Geobacter* as the absolutely dominant genus in the SCMFC anode was eliminated and replaced by *Azonexus* and *Pseudomonas* in the DNMFC. Furthermore, the biomass of *Pseudomonas* (151.0 ng/ μ L) in the DNMFC cathode was five-fold higher than that in the SCMFC, although the bacterial community compositions were quite similar. The DNMFC with highly abundant *Pseudomonas* exhibited much better performance in terms of electrochemical activity and nitrate removal. The evolution process of functional bacteria from the SCMFC to the DNMFC comprehensively reveals the significant role of denitrifying electroactive bacteria in a bioelectrochemical system for nitrogen-containing wastewater treatment.



Citation: Jin, X.; Wang, W.; Yan, Z.; Xu, D. The Important Role of Denitrifying Exoelectrogens in Single-Chamber Microbial Fuel Cells after Nitrate Exposure. *Separations* **2024**, *11*, 187. <https://doi.org/10.3390/separations11060187>

Academic Editor: Sascha Nowak

Received: 13 May 2024

Revised: 3 June 2024

Accepted: 9 June 2024

Published: 14 June 2024



Copyright: © 2024 by the authors. Licensee MDPI, Basel, Switzerland. This article is an open access article distributed under the terms and conditions of the Creative Commons Attribution (CC BY) license (<https://creativecommons.org/licenses/by/4.0/>).

Keywords: microbial fuel cells; nitrogen; denitrification; community evolution; denitrifying electroactive bacteria

1. Introduction

Nitrogen, as one of the main targeted pollutants in wastewater treatment [1], is extensively removed through the A/O process involving aerobic nitrification by autotrophic bacteria and anaerobic denitrification by heterotrophic bacteria [2,3]. This process is characterized as occupying a large area and producing excess sludge, with high energy consumption and costs, which is an unsustainable strategy for the development of the ecological environment. The microbial fuel cell (MFC), especially the single-chamber air cathode MFC (SCMFC), seems to be a high-potential technology for wastewater treatment because it not only provides benefits in terms of direct electricity generation and reduced sludge production but also saves aeration energy and enhances nutrient removal [4,5]. Therefore, the SCMFC has become an amazing technology for nitrogen removal in wastewater treatment [6–8].

As known, SCMFCs can efficiently remove nutrients and nitrogen while enhancing energy recovery through various improvement strategies [9–12]. These strategies generally include the tailoring of the electrode spacing [13] and external resistance [14], solution conductivity or a buffer [15], different chemical oxygen demand (COD)/N wastewaters [16,17], electrode materials [18,19], and catalysts [20,21]. The maximum removal efficiencies of

chemical oxygen demand (COD), NH_4^+ -N, and total nitrogen (TN) are above 90%; meanwhile, the maximum coulombic efficiency (CE) increases to 69.2%. Major studies have remarked that nitrogen removal in SCMFCs is consistent with conventional nitrification and denitrification [22,23]; however, a few researchers have thought that bioelectrochemical denitrification plays a key role in a denitrifying MFC (DNMFC) for low-COD wastewater treatment [24,25].

In a common chamber, the nitrogen removal mechanism in a DNMFC appears to be considerably complex: ammonium is oxidized to nitrite/nitrate by nitrifying bacteria on the cathode, and nitrification products are either reduced through heterotrophic denitrification [26] or via bioelectrochemical denitrification [27]. Further, nitrate reduction by denitrifying bacteria is also accompanied by the consumption of organics as electron donors, which compete with anode respiration [11,26,28]. Therefore, in order to clarify the mechanism of nitrogen removal in the bioelectrochemical system, it is necessary to comprehensively compare the quantitative distribution of nutrients and dominated bacteria between SCMFCs and DNMFCs for nitrogen-containing wastewater treatment.

This study focused on quantifying the distribution of acetate and nitrogen and the exact concentrations of the dominant functional bacteria in MFCs. Therefore, we fabricated a special SCMFC and DNMFC to compare their performances in terms of electrochemical activity and nitrogen removal. Furthermore, the functional bacterial distribution was accurately quantified based on the DNA concentrations. Quantifying the distribution of nutrients and functional microorganisms in SCMFCs and DNMFCs can not only clearly explain the evolution process of the MFC system after nitrate exposure, but can also effectively guide the efficient removal of nitrogen in wastewater.

2. Materials and Methods

2.1. MFC Configuration and Operational Conditions

The single-chamber microbial fuel cell (SCMFC) consisted of a chamber ($\Phi 3 \text{ cm} \times 4 \text{ cm}$) with a total working volume of 30 mL. The anode was composed of a circular carbon cloth (Alfa Aesar, Thermo Fisher Scientific Inc., Waltham, MA, USA) with a diameter of 3.0 cm, which was pre-enriched by hanging on a mature anode in the dual-chamber MFC in long-term stable operation [29]. Poly(dimethylsiloxane) (PDMS, Sylgard 184, Dow Inc., Auburn, MI, USA) was brushed on the blocking layer of a commercial carbon cloth (W1s1009, Phychemi Co., Ltd., Hong Kong, China) as the diffusion layer, and platinum was coated on the other side as the catalyst layer of the cathode [29]. The anode and cathode were placed on opposite sides of the chamber and connected to a 1 k Ω resistor using a titanium wire.

The synthetic wastewater (W1) was composed of 1.0 g/L CH_3COONa , 10.13 g/L Na_2HPO_4 , 6.08 g/L NaH_2PO_4 , 0.13 g/L KCl , 0.31 g/L NH_4Cl , and 12.5 mL/L Wolfe's mineral solution. NaNO_3 instead of NH_4Cl was added into W1 as nitrate-containing wastewater (W2). Then, wastewater was purged with N_2 until the dissolved oxygen (DO) was maintained below 0.2 mg/L and fed into the SCMFC and DNMFC chambers. The system was operated in fed-batch mode at an ambient temperature of $30 \pm 1 \text{ }^\circ\text{C}$. After operation for 15 d, 38 d, and 50 d, polarization curves were tested by varying the external resistance from 10,000 to 10 Ω and measuring the voltage at each resistance. All tests were conducted in duplicate, and parallelization of more than three cycles was tested under identical conditions in each test to ensure the accuracy of the results.

2.2. Analysis

During the stable operation stage, the effluent samples were withdrawn from each batch using a syringe and passed through a syringe filter (0.45 μm pore diameter) before analysis. The concentrations of chemical oxygen demand (COD), NH_4^+ -N, NO_2^- -N, and NO_3^- -N were measured according to the APHA standard methods [30]. The output voltages were recorded at 5 min intervals using a computer with a data acquisition system, as described previously [28]. Power density curves were calculated by varying the external

resistor. The total genomic DNA was extracted from an entire piece of each electrode, and its concentration of nucleic acid was measured to express the electrode biomass. The dominant bacteria in the microbial community were identified by high-throughput sequencing. The quantification of the dominant bacterium was calculated as the percentage multiplied by the total DNA concentration. The charges from the collected electric charge (E_e) by MFCs, the theoretically consumed electric charge for nitrate reduction (EN), and the theoretically generated electric charge by acetate oxidation (EA) were calculated by using the equations presented in the Supporting Information, as well as the coulombic efficiency (CE, %) and electron transfer efficiency (ETE, %).

2.3. Micromorphology Observation and Microbial Community Analysis

The micromorphology of the electrode biofilms was observed by using a scanning electron microscope (SEM) (JSM-6510LV, JEOL Ltd., Tokyo, Japan) and confocal laser scanning microscope (CLSM) (InVia Reflex, Renishaw Plc., Gloucestershire, UK). The sample treatment method before SEM and CLSM is described in the Supporting Information. The V3–V4 regions of the bacterial 16S rDNA were amplified by using the Gene Amp PCR System (Applied Biosystems, Foster City, CA, USA) using the primers 338F (5'-CCTACGGGAGGCAGCAG-3') and 806R (5'-GGACTA CHVGGGTWTCTAAT-3'), where the barcode was an eight-base sequence unique to each sample [31]. The PCR products were sequenced using the MiSeq Illumina platform (Majorbio Bio-pharm Technology, Shanghai, China). The raw data were processed using the Illumina RDP database, and reads were demultiplexed according to the index sequence [28]. The analyzed data were used to express the microbial community distribution of electrode biofilms at the class and genus levels.

3. Results and Discussion

3.1. Performance Evaluation of DNMFC and SCMFC

3.1.1. Electroactivity Performance

Power densities and polarization curves were measured to express the electroactive stability of electrode biofilms in the DNMFC and SCMFC during operation. As shown in Figure 1, similar waves of power density and polarization curves on days 38 and 50 indicate the stability of the operating system and the electrode biofilms. Furthermore, according to the polarization curves, the anode potentials were highly consistent with the increase in current densities, attributed to the pre-enriched biofilm of the anodes before reactor startup. The cathode potential tended to be stable after 38 d, indicating the appearance of stable and mature biofilms on the surface of the Pt/C cathode. Significantly, from the moment of reactor startup, the maximum power density of the DNMFC only decreased by 16.5% from 13.3 ± 0.6 to 11.1 ± 0.8 V/m³ after 50 days, whereas that of the SCMFC reduced by more than 41.3% (declined from 12.1 ± 0.3 to 7.1 ± 0.4 V/m³). The considerable difference between the DNMFC and SCMFC was attributed to the cathode potential decay rather than the anode potentials, implying the presence of a more highly electroactive biofilm on the DNMFC cathode.

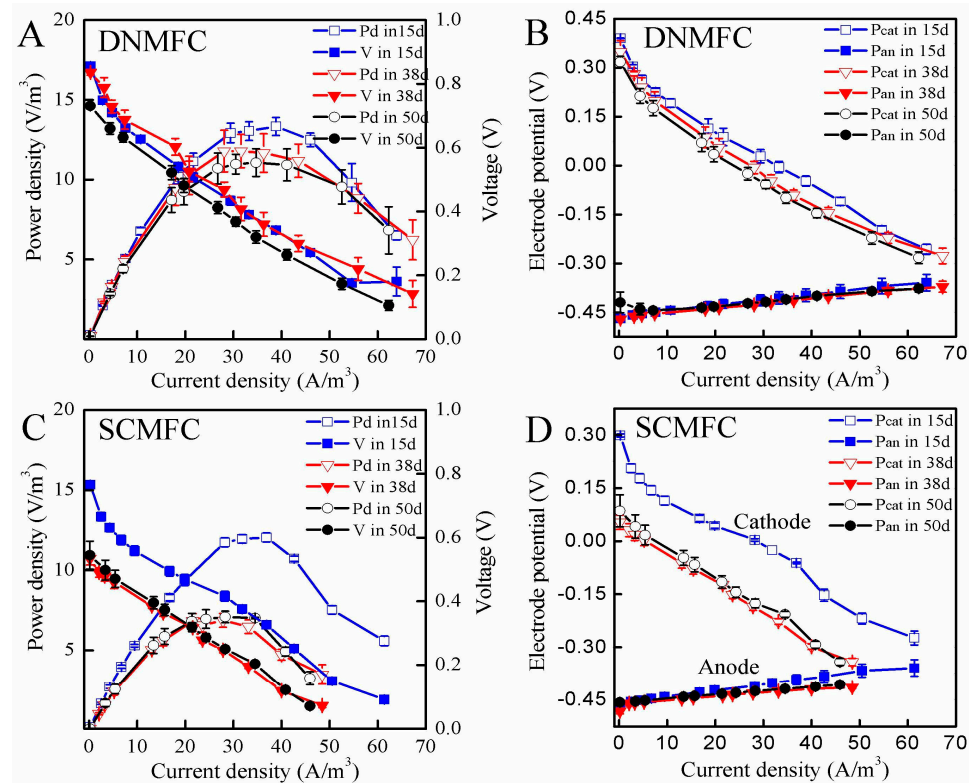


Figure 1. Power densities (A,C) and electrode polarization curves (B,D) of MFCs for different incubation times. DNMFC (A,B); SCMFC (C,D).

3.1.2. Voltage Variation and Nitrogen Removal

On the other hand, electron recovery and nitrogen removal abilities were exhibited by MFCs with the W1 and W2 treatments (Figure 2 and Table 1). To begin with, the cycle time of MFCs in the presence of NH_4^+ was approximately two times longer than that in the presence of NO_3^- . Therefore, the relative electron recovery of the DNMFC and SCMFC sharply decreased from 106.8 ± 0.3 to $46.7 \pm 0.2 \mu\text{mol}/\text{e}$ and from 127.3 ± 0.3 to $36.2 \pm 4.5 \mu\text{mol}/\text{e}$, respectively. Additionally, the NH_4^+ losses in the DNMFC and SCMFC were only 6.2% and 13.5%, respectively; furthermore, a null concentration of NO_2^- and NO_3^- was detected in the bulk solution throughout cycle operation, indicating that ammonium oxidation did not occur on the air cathode surface (Figure 2B). The voltage in the SCMFC gradually decreased and remained constant throughout the DNMFC cycle, implying that nitrogen significantly influenced the voltage stability in the SCMFC. Last but not least, significant differences in the route of NO_3^- reduction were notably observed in the DNMFC and SCMFC. In the DNMFC, NO_3^- was rapidly reduced, with no noticeable accumulation of intermediates during the entire process, demonstrating the efficient biological denitrification by denitrifying bacteria [32]. However, distinct accumulations of NO_2^- and NH_4^+ were observed in the SCMFC, implying that NO_3^- was removed by converting it to N_2 or ammonia via dissimilatory nitrate reduction [33]. In the SCMFC, the removal rates of NO_3^- and total nitrogen were $80.3 \pm 2.0\%$ and $65.0 \pm 3.5\%$, respectively, which were considerably lower than those in the DNMFC. Similarly, the DNMFC exhibited a higher COD removal ability than the SCMFC, implying that nitrate reduction also promoted organic matter removal.

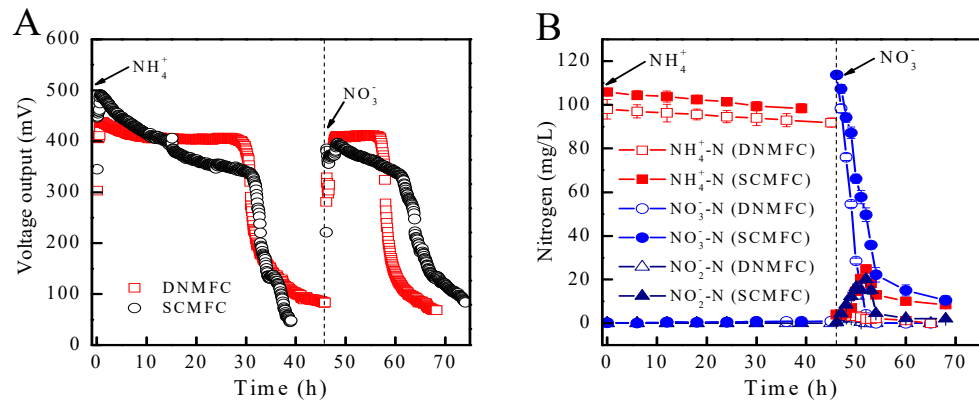


Figure 2. Voltage outputs and nitrogen concentration changes in DNMFC and SCMFC with NH₄⁺/NO₃⁻-containing wastewater treatment.

Table 1. Comparisons of energy recovery and nitrogen removal in SCMFC and DNMFC under NH₄⁺ or NO₃⁻-containing conditions.

	DNMFC	SCMFC
Electron recovery (NH ₄ ⁺)	106.8 ± 0.3	127.3 ± 0.3
NH ₄ ⁺ -N loss	6.2 ± 0.5%	13.5 ± 1.0%
NO ₃ ⁻ -N generation	0.3 ± 0.1%	n.d. ¹
COD removal	93.4 ± 0.2	87.4 ± 0.4%
Electron recovery (NO ₃ ⁻)	46.7 ± 0.2	36.2 ± 4.5
NO ₃ ⁻ -N removal	99.2 ± 1.0%	80.3 ± 2.0%
NO ₂ ⁻ -N generation	0.03 ± 0.01%	4.9 ± 0.2%
NH ₄ ⁺ -N generation	0.1 ± 0.2%	11.4 ± 1.2%
TN removal	98.1 ± 0.2%	65.0 ± 3.5%
COD removal	95.4 ± 0.2%	89.3 ± 0.5%

n.d.¹ means that the NO₃⁻-N concentration is below the detection limit.

3.1.3. Performance of DNMFC

The electron fluxes in the DNMFC were also investigated at COD/NO₃⁻ ratios from 8 to 3.6 (Figure 3 and Table 2). NO₃⁻ was majorly removed when the COD/NO₃⁻ ratio was above 4.3, which was quite close to that of 3.5 for removal by heterotrophic denitrifying bacteria [1]. Therefore, compared to traditional biological denitrification in wastewater treatment, bioelectrochemical systems (BESs) for nitrogen removal have the advantages of a lower production of active sludge, high efficiency, and energy recovery. Compared to the electroactivity and electricity generation in BESs, the CE of 38.0 ± 1.1% in the DNMFC was slightly lower than that of 45.3 ± 0.8% in the SCMFCs, in the absence of NO₃⁻. CEs sharply declined with a decrease in the COD/NO₃⁻ ratio, whereas ETEs increased from 52.5 ± 0.5% to 71.1 ± 0.8% and then decreased to 44.2 ± 0.5% at a COD/NO₃⁻ ratio of 3.6. Under the conditions of insufficient organic matter, the intermediates of NH₄⁺ considerably accumulated, suggesting the presence of electrochemical nitrate reduction to ammonia in the DNMFC.

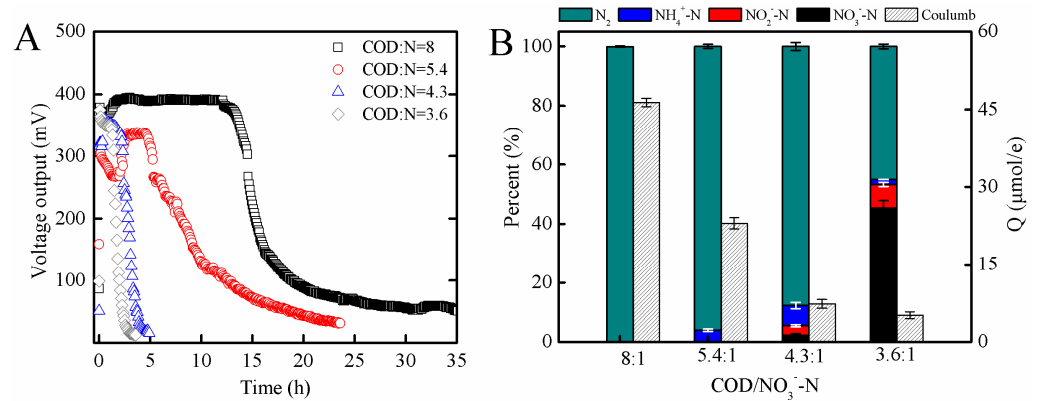


Figure 3. Voltage outputs (A), nitrogen distribution, and the collected electric charge (B) of DNMFCs at different COD/NO₃⁻-N ratios.

Table 2. Comparison of electron transfer efficiency in DNMFC under different COD/NO₃⁻-N ratios.

COD/NO ₃ ⁻ -N	E _A ¹ (μmol/e)	Ee ² (μmol/e)	E _N ³ (μmol/e)	CE (%)	ETE (%)
8:0	281.1 ± 3.5	106.8 ± 4.5	/	38.0 ± 1.1	38.0 ± 1.1
8:1	281.1 ± 2.5	46.4 ± 2.0	101.2 ± 1.2	16.5 ± 0.5	52.5 ± 0.5
5.4:1	210.8 ± 2.8	23.0 ± 1.2	115.3 ± 1.5	10.9 ± 0.5	65.6 ± 0.5
4.3:1	168.7 ± 2.1	7.3 ± 0.6	112.6 ± 1.0	4.3 ± 0.8	71.1 ± 0.8
3.6:1	140.5 ± 1.7	5.2 ± 0.5	56.9 ± 0.5	3.7 ± 0.5	44.2 ± 0.5

¹ Theoretically generated electrical charge of acetate; ² collected electric charge from current generation; ³ theoretically consumed electric charge for nitrate reduction.

3.2. Microbial Community Analysis of DNMFC and SCMFC

The surface morphology of the electrodes showed that bacteria were densely distributed on the carbon fiber of the anode and the Pt/C nanoparticles of the cathode to form a thin biofilm (Figure S1). Based on Illumina sequencing, the bacterial community diversity in the DNMFC and SCMFC was investigated at the genus level (Figure 4). The observed bacterial community compositions differed significantly, especially in the anode. *Geobacter*, a model genus of electroactive bacteria (EAB), was widely found in acetate-fed BESs [32–34]. In this study, *Geobacter*, which was the most dominant genus in the SCMFC anode (accounting for 63.7%), practically disappeared in the DNMFC. In contrast, the bacterial communities of the DNMFC were dominated by *Azonexus* (33.1%), *Pseudomonas* (17.6%), and *Comamonas* (10.7%), which are usually identified as chemoheterotrophic denitrifiers (DNBs) and denitrifying exoelectrogens (DENBs) [35–37]. Moreover, other genera related to nitrate reduction, such as *Rhodocyclus*, *Azoarcus*, *Chryseobacterium*, *Ignavibacterium*, and *Aminiphilus*, were also dominant in the system and mainly involved in the microbial degradation of organic matter and nitrogen [8,38].

Interestingly, similar compositions of the bacterial community were notably found in the cathode of the DNMFC and SCMFC but at different abundances. *Pseudomonas* species, which are identified as DENBs [39], accounted for 49.6% and 29.4% of the bacteria in the DNMFC and SCMFC, respectively. It seems that the addition of nitrate enriched the DNBs in the DNMFC, and the few species that adhered to the cathode surface were involved in the extracellular electron transfer on the cathode [34]. Thus, compared to the SCMFC, the cathode biofilm in the DNMFC displayed an increased DENB abundance, which partly compensated for the active site reduction of Pt/C. The oxygen reduction reaction (ORR) using a chemical catalyst of Pt/C can be performed in a series of reactions with the cooperation of Pt/C, DNBs, and DENBs. Compared to the metal-free carbon cloth used as a cathode, the metal-coated cathode in the SCMFC had a shorter startup time, with higher bioelectrochemical activity and nitrogen removal efficiency [8].

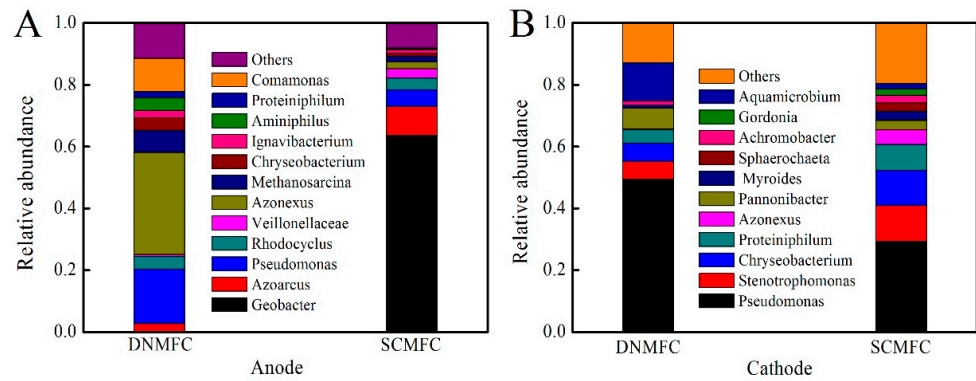


Figure 4. Microbial community analysis of the anode (A) and cathode (B) at the genus level in the DNMFC and SCMFC.

3.3. Quantitative Analysis of Functional Bacteria

The biomass densities of the SCMFC and DNMFC considerably differed when viewed through a scanning electron microscope (Figure S2). The anode biofilm biomass of the DNMFC expressed by the total DNA concentration was $145.1 \pm 5.5 \text{ ng}/\mu\text{L}$, which was slightly lower than that of the SCMFC at $197.1 \pm 5.1 \text{ ng}/\mu\text{L}$. Conversely, the cathode biofilm biomass of the DNMFC ($306.4 \pm 13.5 \text{ ng}/\mu\text{L}$) was approximately three times thicker than that of the SCMFC ($109.7 \pm 7.1 \text{ ng}/\mu\text{L}$). Furthermore, when viewed at a macroscopic level, the biomass in the solution significantly differed between the DNMFC and SCMFC (Figure S1). The DNMFC solution was slightly turbid, whereas the SCMFC solution was clear, implying that nitrate induced microbial metabolism in the solution and subsequently increased the cathode biofilm biomass.

According to the total DNA of the samples and the relative abundance of each dominant genus, the biomass was quantitatively determined, and the change trends achieved between the SCMFC and DNMFC were identified (Figure 5). The dominant genera of the anode biofilm in the DNMFC were in the order of *Azonexus*, *Pseudomonas*, *Comamonas*, *Chryseobacterium*, and *Aminiphilus*, which are considered DNBs and EAB. However, the single most dominant genus on the SCMFC anode was *Geobacter*, which reached $125.6 \text{ ng}/\mu\text{L}$ and accounted for 63.7%. The genus *Azonexus* dominated the anode of the DNMFC with a high relative abundance of 33.1%, which practically disappeared in the cathode biofilm, implying that *Azonexus* as an alternative DNB needs anaerobic conditions for growth. In contrast, few aerobic bacteria (including *Aquamicrobium* and *Azoarcus*) exhibited remarkably high relative abundances in the cathode chamber, consuming O_2 permeating from the air cathode, thereby making the cathode a hypoxic environment suitable for the growth of denitrifiers.

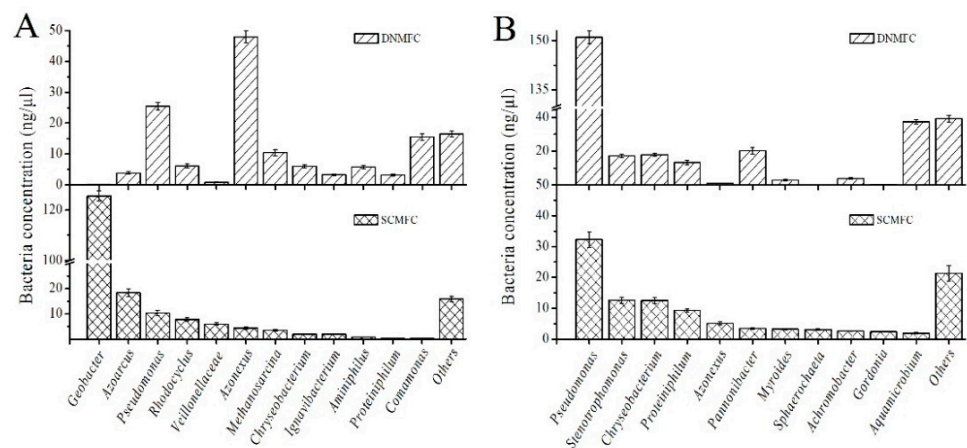


Figure 5. Comparisons of bacterial concentrations in anodes (A) and cathodes (B) of DNMFC and SCMFC.

The *Pseudomonas* biomass of 151.0 ng/ μ L in the DNMFC cathode was five-fold higher than that in the SCMFC, confirming the involvement of DENBs in nitrate reduction and cathode electron transfer. The high abundance absolutely dominated the cathode microbial community, indicating that this special genus remarkably reduced nitrate through heterotrophic/electrochemical denitrification [28,40]. Additionally, the biomasses of other dominant genera, except for *Aquamicrobium* [40] and *Pannonibacter* [41], were rather similar between the DNMFC and SCMFC, which may be related to the inoculum. These results proved that the good performance of the DNMFC benefited from the cooperation of nitrogen-removing bacteria. In brief, for nitrate reduction, the DNMFC with nitrate exhibited higher values for functional abundance compared to that of the SCMFC, which enhances the simultaneous electricity generation and denitrifying process in nitrogen-containing wastewater treatment [28]. During long-term operations of the DNMFC, when observed using CLSM, copious amounts of bacteria in the inner layer of the electrode biofilms died (Figure 6), demonstrating that the inner layer of the thick biofilm could not satisfy the nutrient demand in the oligotrophic micro-environment [34].

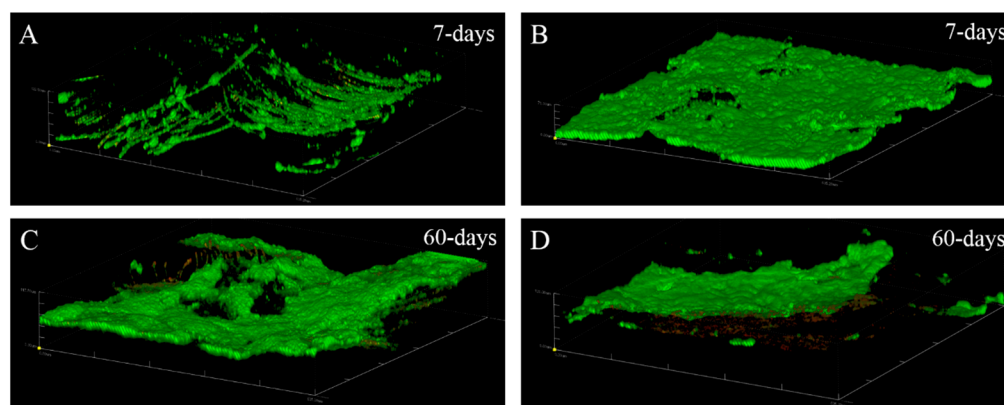


Figure 6. CLSM of proteins within the interior layers of electrode biofilms in the DNMFC after 7 d (A,B) and 60 d (C,D) of operation. (A,C) are the anodes of the DNMFC; (B,D) are the cathodes of the DNMFC.

3.4. Insights into the Evolution Process after Nitrate Exposure

According to the above results, the microbial community evolution process in the single-chamber MFC following nitrate exposure can be described. The community structure of the anode biofilm was relatively simple; *Geobacter* was absolutely dominant in the acetate-fed SCMFC [28,34]. However, *Azonexus* and *Pseudomonas*, which are known DNBs and DENBs, prefer to grow in nitrogen-containing solutions, replacing *Geobacter* and becoming the new dominant species in DNMFCs [8,35,42]. Nitrate stimulates the growth of nitrogen-metabolizing bacteria, resulting in DNB enrichment, with a remarkable ecological impact on DNMFCs [26,43].

When considering both the relative abundances and total biomass in the test system, the compositions of the dominant genera from the SCMFC to DNMFC were comprehensively analyzed. In this study, the functional bacteria can be grouped into three categories: DNB, EAB, and DENB. First, DNBs were rapidly accumulated in the solution and then adhered to the electrodes after nitrate exposure. Second, EAB that could adapt to the nitrate-containing aqueous environment were either retained (such as *Ignavibacterium*, *Rhodocyclus*, and *Desulfomonile*) or gradually eliminated (for example *Geobacter*) during system operation [11]. Finally, the relative abundance of *Pseudomonas* increased considerably in both the cathode and anode biofilms, which identified its capacity to metabolize nitrogen and transfer electrons. Previous studies have confirmed that *Pseudomonas* is widespread in the electrode, which contains nitrate-reducing species [28,39]. In this system, *Pseudomonas* was related to simultaneous nitrate reduction and electron transfer, consistent with a previous study [28].

Compared to the DNMFC, the relative abundance of EAB, especially *Geobacter*, was high in the SCMFC anode, whereas the cathode biomass remarkably increased based on the similar microbial community structure. Therefore, nitrate exposure not only influences the microbial community structure, but also enriches the relative functional bacteria, resulting in an increase in the cathode biofilm biomass [39]. Despite the promising results achieved in the DNMFC, the scalability and stability of microbial communities after long-term operation should be investigated in further research. Furthermore, maintenance requirements and performance under variable real-world conditions must also be addressed to fully realize the potential of MFC technology in practical applications.

4. Conclusions

This study first compared the performance of SCMFCs and DNMFCs on nitrogen-containing wastewater treatment and comprehensively elucidated the response of the SCMFC to nitrate exposure, revealing the distribution of nutrients and functional bacteria in DNMFCs. Though energy recovery decreased by 22.5% from the SCMFC to the DNMFC for partial electron donors consumed by heterotrophic denitrification, the electron transfer efficiency increased from 38.0% to 52.5%. At the same time, *Geobacteria* was the most dominant genus in the SCMFC anode, while it was eliminated and replaced by *Azonexus* and *Pseudomonas* in the DNMFC. The biomass of *Pseudomonas* (151.0 ng/ μ L) in the DNMFC cathode was five-fold higher than that in the SCMFC, though the bacterial community compositions were quite similar. The DNMFC with highly abundant *Pseudomonas* exhibited much better performance in terms of electrochemical activity and nitrogen removal following nitrate exposure. This microbial community evolution comprehensively reveals the significant role of denitrifying electroactive bacteria in bioelectrochemical systems for nitrogen-containing wastewater treatment.

Supplementary Materials: The following supporting information can be downloaded at: <https://www.mdpi.com/article/10.3390/separations11060187/s1>. The calculation formula for electric transfer and the treatment methods of electrodes for SEM and CLSM were listed in the Supporting Informations. The physical images of reactors and electrodes in DNMFC and SCMFC were shown in Figure S1. The microbial morphology of electrodes were shown in Figure S2.

Author Contributions: Conceptualization, X.J. and D.X.; methodology, X.J. and W.W.; software, Z.Y.; validation, X.J. and W.W.; formal analysis, X.J. and W.W.; investigation, X.J.; resources, X.J. and D.X.; data curation, X.J.; writing—original draft preparation, X.J.; writing—review and editing, X.J., W.W. and Z.Y.; visualization, X.J.; supervision, D.X.; project administration, X.J.; funding acquisition, X.J. All authors have read and agreed to the published version of the manuscript.

Funding: This research work was financially supported by the National Natural Science Foundation of China (Nos. 52000169, 52131003).

Data Availability Statement: Data are contained within the article and Supplementary Materials.

Acknowledgments: The authors are grateful to Nuan Yang and Hong Liu for their help with the revision of figures in this paper and the useful suggestion for the paper. We also thank the associate editor and the reviewers for their useful feedback that improved this paper.

Conflicts of Interest: The authors declare no conflicts of interest.

References

1. Modin, O.; Fukushi, K.; Rabaey, K.; Rozendal, R.A.; Yamamoto, K. Redistribution of wastewater alkalinity with a microbial fuel cell to support nitrification of reject water. *Water Res.* **2011**, *45*, 2691–2699. [[CrossRef](#)]
2. Knowles, R. Denitrification. *Microbiol. Rev.* **1982**, *46*, 43–70. [[CrossRef](#)] [[PubMed](#)]
3. Sun, S.-P.; Nàcher, C.P.I.; Merkey, B.; Zhou, Q.; Xia, S.-Q.; Yang, D.-H.; Sun, J.-H.; Smets, B.F. Effective Biological Nitrogen Removal Treatment Processes for Domestic Wastewaters with Low C/N Ratios: A Review. *Environ. Eng. Sci.* **2010**, *27*, 111–126. [[CrossRef](#)]
4. Yan, H.J.; Saito, T.; Regan, J.M. Nitrogen removal in a single-chamber microbial fuel cell with nitrifying biofilm enriched at the air cathode. *Water Res.* **2012**, *46*, 2215–2224. [[CrossRef](#)]

5. Rossi, R.; Hur, A.Y.; Page, M.A.; Thomas, A.O.B.; Butkiewicz, J.J.; Jones, D.W.; Baek, G.; Saikaly, P.E.; Cropek, D.M.; Logan, B.E. Pilot scale microbial fuel cells using air cathodes for producing electricity while treating wastewater. *Water Res.* **2022**, *215*, 118208. [[CrossRef](#)]
6. Chen, L.; Ding, C.; Liu, B.; Lian, J.; Lai, L.; Yuan, L.; Wang, R. A Promising Process to Remove Nitrate from Solar Panel Production Wastewater and Meanwhile Generating Electricity. *Water* **2023**, *15*, 3347. [[CrossRef](#)]
7. Liu, W.F.; Cheng, S.A.; Yin, L.; Sun, Y.; Yu, L.L. Influence of soluble microbial products on the long-term stability of air cathodes in microbial fuel cells. *Electrochim. Acta* **2018**, *261*, 557–564. [[CrossRef](#)]
8. Yang, J.W.; Cheng, S.A. Effects of Using Anode Biofilm and Cathode Biofilm Bacteria as Inoculum on the Start-up, Electricity Generation, and Microbial Community of Air-Cathode Single-Chamber Microbial Fuel Cells. *Pol. J. Environ. Stud.* **2019**, *28*, 693–700.
9. Li, H.; Zuo, W.; Tian, Y.; Zhang, J.; Di, S.J.; Li, L.P.; Su, X.Y. Simultaneous nitrification and denitrification in a novel membrane bioelectrochemical reactor with low membrane fouling tendency. *Environ. Sci. Pollut. Res.* **2017**, *24*, 5106–5117. [[CrossRef](#)]
10. Yang, N.; Zhan, G.Q.; Luo, H.; Xiong, X.; Li, D.P. Integrated simultaneous nitrification/denitrification and comammox consortia as efficient biocatalysts enhance treatment of domestic wastewater in different up-flow bioelectrochemical reactors. *Bioresour. Technol.* **2021**, *339*, 125604. [[CrossRef](#)]
11. Yang, N.; Zhou, Q.M.; Zhan, G.Q.; Liu, Y.L.; Luo, H.Q.; Li, D.P. Comparative evaluation of simultaneous nitrification/denitrification and energy recovery in air-cathode microbial fuel cells (ACMFCs) treating low C/N ratio wastewater. *Sci. Total Environ.* **2021**, *788*, 147652. [[CrossRef](#)] [[PubMed](#)]
12. Zhang, L.F.; Wang, J.Q.; Fu, G.K.; Zhang, Z. Simultaneous electricity generation nitrogen carbon removal in single-chamber microbial fuel cell for high-salinity wastewater treatment. *J. Clean. Prod.* **2020**, *276*, 123203. [[CrossRef](#)]
13. Park, Y.; Nguyen, V.; Park, S.; Yu, J.; Lee, T. Effects of anode spacing and flow rate on energy recovery of flat-panel air-cathode microbial fuel cells using domestic wastewater. *Bioresour. Technol.* **2018**, *258*, 57–63. [[CrossRef](#)] [[PubMed](#)]
14. Pinto, R.P.; Srinivasan, B.; Guiot, S.R.; Tartakousky, B. The effect of real-time external resistance optimization on microbial fuel cell performance. *Water Res.* **2011**, *45*, 1571–1578. [[CrossRef](#)] [[PubMed](#)]
15. Nam, J.Y.; Kim, H.W.; Lim, K.H.; Shin, H.S.; Logan, B.E. Variation of power generation at different buffer types and conductivities in single chamber microbial fuel cells. *Biosens. Bioelectron.* **2010**, *25*, 1155–1159. [[CrossRef](#)] [[PubMed](#)]
16. Castro, C.J.; Taha, K.; Kenney, I.; Yeh, D.H. The Role of Carbon to Nitrogen Ratio on the Performance of Denitrifying Biocathodes for Decentralized Wastewater Treatment. *Water* **2022**, *14*, 3076. [[CrossRef](#)]
17. Kong, Y.; Hu, J.; Lu, X.; Cheng, C. Effects of Carb on Source on Denitrification and Electricity Generation in Composite Packing MFC-CW for Tail Water Treatment. *Water* **2023**, *15*, 4285. [[CrossRef](#)]
18. Mei, T.; Cong, C.; Huang, Q.; Song, T.S.; Xie, J.J. Effect of 3D Carbon Electrodes with Different Pores on Solid-Phase Microbial Fuel Cell. *Energ. Fuels* **2020**, *34*, 16765–16771. [[CrossRef](#)]
19. Zhang, X.L.; Li, C.H.; Guo, Q.J.; Huang, K.L. Performance of anaerobic fluidized bed microbial fuel cell with different porous anodes Chinese. *J. Chem. Eng.* **2020**, *28*, 846–853.
20. Dessie, Y.; Tadesse, S.; Eswaramoorthy, R.; Adimasu, Y. Biosynthesized alpha-MnO₂-based polyaniline binary composite as efficient bioanode catalyst for high-performance microbial fuel cell. *All Life* **2021**, *14*, 541–568. [[CrossRef](#)]
21. Liang, B.L.; Ren, C.; Zhao, Y.B.; Li, K.X.; Lv, C.C. Nitrogenous mesoporous carbon coated with Co/Cu nanoparticles modified activated carbon as air cathode catalyst for microbial fuel cell. *J. Electroanal. Chem.* **2020**, *860*, 113904. [[CrossRef](#)]
22. Gurung, A.; Thapa, B.S.; Ko, S.-Y.; Ashun, E.; Toor, U.A.; Oh, S.-E. Denitrification in Microbial Fuel Cells Using Granular Activated Carbon as an Effective Biocathode. *Energies* **2023**, *16*, 709. [[CrossRef](#)]
23. Kondaveeti, S.; Choi, D.-H.; Noori, M.T.; Min, B. Ammonia Removal by Simultaneous Nitrification and Denitrification in a Single Dual-Chamber Microbial Electrolysis Cell. *Energies* **2022**, *15*, 9171. [[CrossRef](#)]
24. Zhang, F.; He, Z. Integrated organic and nitrogen removal with electricity generation in a tubular dual-cathode microbial fuel cell. *Process Biochem.* **2012**, *47*, 2146–2151. [[CrossRef](#)]
25. Zhang, R.; Wu, Y.; Wang, L.T.; Wu, Q.; Zhang, H.W. Cathode Denitrification of Microbial Fuel Cells. *Prog. Chem.* **2020**, *32*, 2013–2021.
26. Huang, H.B.; Cheng, S.A.; Yang, J.W.; Li, C.C.; Sun, Y.; Cen, K.F. Effect of nitrate on electricity generation in single-chamber air cathode microbial fuel cells. *Chem. Eng. J.* **2018**, *337*, 661–670. [[CrossRef](#)]
27. Qiao, S.; Yin, X.; Zhou, J.T.; Wei, L.E.; Zhong, J.Y. Integrating anammox with the autotrophic denitrification process via electrochemistry technology. *Chemosphere* **2018**, *195*, 817–824. [[CrossRef](#)]
28. Jin, X.J.; Guo, F.; Ma, W.Q.; Liu, Y.; Liu, H. Heterotrophic anodic denitrification improves carbon removal and electricity recovery efficiency in microbial fuel cells. *Chem. Eng. J.* **2019**, *370*, 527–535. [[CrossRef](#)]
29. Gao, Y.Y.; Wang, S.; Yin, F.J.; Hu, P.; Wang, X.Z.; Liu, Y.; Liu, H. Enhancing sensitivity of microbial fuel cell sensors for low concentration biodegradable organic matter detection: Regulation of substrate concentration anode area external resistance. *J. Environ. Sci.* **2021**, *101*, 227–235. [[CrossRef](#)]
30. American Public Health Association (APHA). *Standard Methods for Examination of Water and Wastewater*, 21st ed.; Water Environment Federation: Washington, DC, USA, 2001.
31. Vilar-Sanz, A.; Puig, S.; Garcia-Lledo, A.; Trias, R.; Balaguer, M.D.; Colprim, J.; Baneras, L. Denitrifying Bacterial Communities Affect Current Production and Nitrous Oxide Accumulation in a Microbial Fuel Cell. *PLoS ONE* **2013**, *8*, e63460. [[CrossRef](#)]

32. Luo, S.; Fu, B.Y.; Liu, F.B.; He, K.; Yang, H.; Ma, J.J.; Wang, H.; Zhang, X.Y.; Liang, P.; Huang, X. Construction of innovative 3D-weaved carbon mesh anode network to boost electron transfer and microbial activity in bioelectrochemical system. *Water Res.* **2020**, *172*, 115493. [[CrossRef](#)]
33. Kashima, H.; Regan, J.M. Facultative nitrate reduction by electrode-respiring *Geobacter metallireducens* biofilms as a competitive reaction to electrode reduction in a bioelectrochemical system. *Environ. Sci. Technol.* **2015**, *49*, 3195–3202. [[CrossRef](#)]
34. Yuan, J.Q.; Yuan, H.G.; Huang, S.B.; Liu, L.J.; Fu, F.C.; Zhang, Y.Q.; Cheng, F.Q.; Li, J.F. Comprehensive performance, bacterial community structure of single-chamber microbial fuel cell affected by COD/N ratio and physiological stratifications in cathode biofilm. *Bioresour. Technol.* **2021**, *320*, 124416. [[CrossRef](#)] [[PubMed](#)]
35. Jangir, Y.; French, S.; Momper, L.M.; Moser, D.P.; Amend, J.P.; El-Naggar, M.Y. Isolation and Characterization of Electrochemically Active Subsurface Delftia and Azonexus Species. *Front. Microbiol.* **2016**, *7*, 756. [[CrossRef](#)] [[PubMed](#)]
36. Manogari, R.; Daniel, D.K. Isolation, Characterization and Assessment of *Pseudomonas* sp. VITDM1 for Electricity Generation in a Microbial Fuel Cell. *Indian J. Microbiol.* **2015**, *55*, 8–12. [[CrossRef](#)]
37. Xing, D.F.; Cheng, S.A.; Logan, B.E.; Regan, J.M. Isolation of the exoelectrogenic denitrifying bacterium *Comamonas denitrificans* based on dilution to extinction. *Appl. Microbiol. Biot.* **2010**, *85*, 1575–1587. [[CrossRef](#)] [[PubMed](#)]
38. Li, W.Y.; Liu, Y.X.; Wu, L.J.; Ren, R.P.; Lv, Y.K. Enhanced nitrogen removal of low C/N wastewater using a novel microbial fuel cell (MFC) with *Cupriavidus* sp. S1 as a biocathode catalyst (BCS1). *J. Chem. Technol. Biot.* **2020**, *95*, 1203–1215. [[CrossRef](#)]
39. Ilamathi, R.; Sheela, A.M.; Gandhi, N.N. Comparative evaluation of *Pseudomonas* species in single chamber microbial fuel cell with manganese coated cathode for reactive azo dye removal. *Int. Biodeterior. Biodegrad.* **2019**, *144*, 104744. [[CrossRef](#)]
40. Li, Z.H.; Zhang, Q.H.; Jiang, Q.R.; Zhan, G.Q.; Li, D.P. The enhancement of iron fuel cell on bio-cathode denitrification and its mechanism as well as the microbial community analysis of bio-cathode. *Bioresour. Technol.* **2019**, *274*, 1–8. [[CrossRef](#)]
41. Sun, Q.; Li, Z.L.; Wang, Y.Z.; Yang, C.X.; Chung, J.S.; Wang, A.J. Cathodic bacterial community structure applying the different co-substrates for reductive decolorization of Alizarin Yellow R. *Bioresour. Technol.* **2016**, *208*, 64–72. [[CrossRef](#)]
42. Yun, H.; Liang, B.; Kong, D.Y.; Wang, A.J. Improving biocathode community multifunctionality by polarity inversion for simultaneous bioelectroreduction processes in domestic wastewater. *Chemosphere* **2018**, *194*, 553–561. [[CrossRef](#)] [[PubMed](#)]
43. Jin, X.J.; Yang, N.; Liu, Y.; Guo, F.; Liu, H. Bifunctional cathode using a biofilm and Pt/C catalyst for simultaneous electricity generation and nitrification in microbial fuel cells. *Bioresour. Technol.* **2020**, *306*, 123120. [[CrossRef](#)] [[PubMed](#)]

Disclaimer/Publisher's Note: The statements, opinions and data contained in all publications are solely those of the individual author(s) and contributor(s) and not of MDPI and/or the editor(s). MDPI and/or the editor(s) disclaim responsibility for any injury to people or property resulting from any ideas, methods, instructions or products referred to in the content.